iScience

CellPress
OPEN ACCESS

Article

Charcoal evidence traces diverse fungal metabolic strategies to the Late Paleozoic

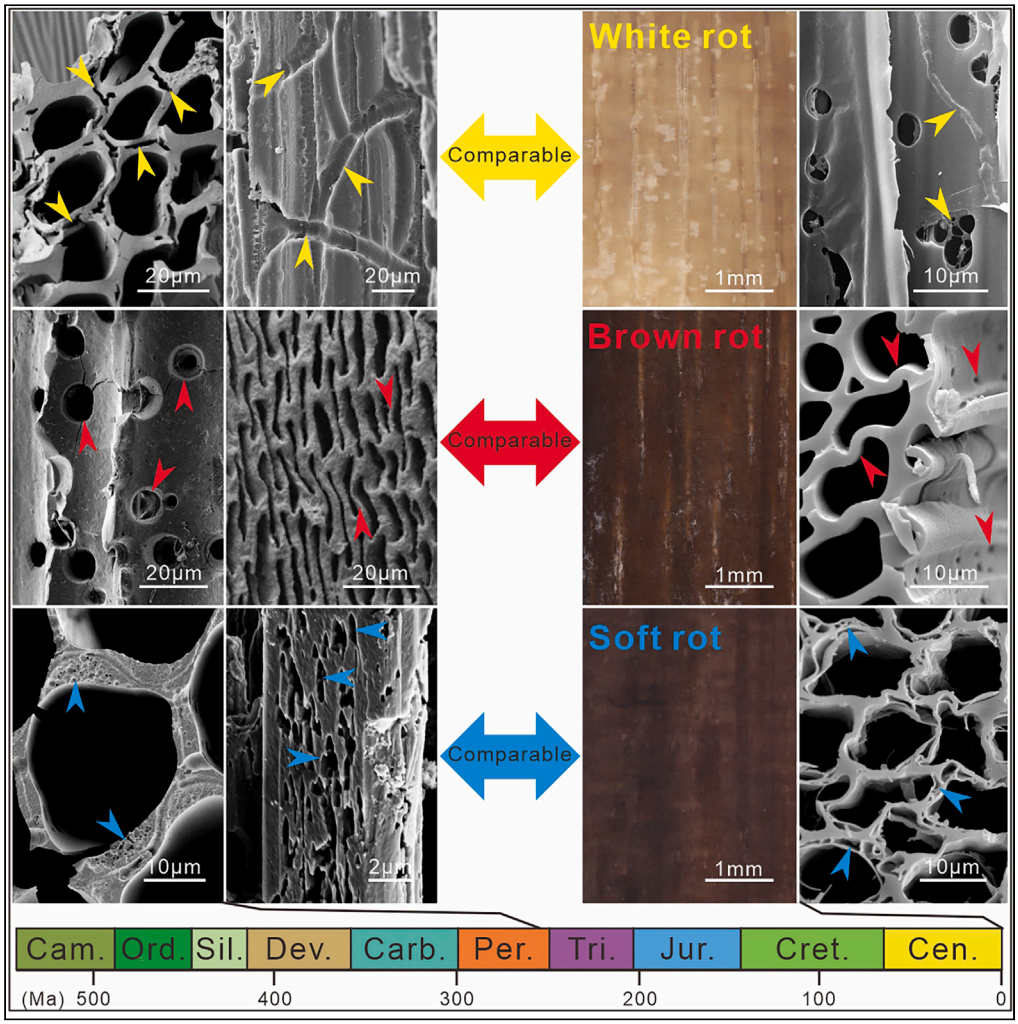

Yaofeng Cai, Hua Zhang, Biao Pan

hzhang@nigpas.ac.cn

Highlights

Wood-decay structures are common in Permian charcoals

Three wood-rotting types can be identified in Permian charcoals

Brown rot and soft rot are evidently traced back to the Late Permian

Wood-decay fungi have developed multiple metabolic strategies by the Late Paleozoic

Cai et al., iScience 27, 110000
June 21, 2024
https://doi.org/10.1016/j.isci.2024.110000

iScience

CellPress
OPEN ACCESS

Article

Charcoal evidence traces diverse fungal metabolic strategies to the Late Paleozoic

Yaofeng Cai,[1] Hua Zhang,[1,3,*] and Biao Pan[2]

SUMMARY

Wood decomposition through fungal activity is essential to the natural carbon cycle. There are three primary patterns of wood decay: white rot, brown rot, and soft rot. However, geological records of wood decay mainly originate from fossil woods, which exclusively describe white rot before the Cenozoic. Fossilized charcoal is another excellent medium for preserving pre-charring decay structures. In this study, we collected numerous charcoals from the upper Permian and observed multiple microstructures indicative of wood decay. The distinctive characteristics closely resemble the symptoms of contemporary wood-rotting types, including the removal of the middle lamella and channel-like lysis seen in white rot, shot-like holes and wavy cell walls in brown rot, and cavities within the secondary walls in soft rot. This study documents the early occurrences of multiple wood-rotting types during the Late Paleozoic and provides insights into the range of fungal metabolic strategies employed during this period.

INTRODUCTION

Microorganisms such as bacteria and fungi are major biomass decomposers in nature and play a critical role in maintaining global nutrient cycles. In particular, fungal decomposition of woody biomass is essential for the continuity of life on Earth,[1] as most microorganisms are unable to decompose lignified tissues in plants, except for white rot fungi, some Ascomycotina, and fungi imperfecti.[2]

Typical woody cell walls have complex structures with varying compositions that confer resistance of pathogens and physical protection. From the exterior to the inside of a typical gymnospermous tracheid, the cell wall comprises a middle lamella (mainly composed of pectin and lignin), a primary wall (made up of hemicellulose, pectin, and subordinately lignin and cellulose), and a three-layered secondary wall (with increasing cellulose, decreasing hemicellulose and pectin, and subordinately lignin).[3] Fungi have evolved various degradation mechanisms targeting specific substrates, which lead to distinct morphological and anatomical structures in decay wood.[4,5] Three principal wood-decay patterns (i.e., white rot, brown rot, and soft rot) have been identified based on the causative fungi and specific decay structures.[1,3] Among these rot types, white rot is mainly caused by basidiomycetes and some ascomycetes, which can produce various enzymes to degrade lignin, cellulose, and hemicellulose.[1,3,4] White rot is known for a wide variety of wood-decay patterns, all of which produce a white color in the wood due to substantial lignin modification or removal from the cells and cellulose bleaching. White rot can be subdivided into two types: preferential delignification, wherein lignin is degraded before polysaccharides,[1] and simultaneous rot, wherein all cell wall components are degraded at the same rate.[5] The former is represented by *Heterobasidion annosum*, *Ceriporiopsis subvermispora*, *Dichomitus squalens*, etc., whereas common fungi that cause simultaneous white rot include *Fomes fomentarius*, *Phellinus igniarius*, *P. robustus*, and so on, in standing trees and stored hardwoods.[1,3] Brown rot is caused by specialized basidiomycetes that lack lignin-degrading enzymes and selectively and completely remove cellulose and hemicelluloses from woody cell walls while leaving behind modified lignin,[1,3,4] which is brown in color, hence the name. As a result of cellulose depolymerization, brown-rotted wood has a high lignin content but little residual strength.[6] Soft rot is caused by ascomycetes and deuteromycetes, which preferentially degrade cellulose and hemicellulose while consuming a limited amount of lignin.[1,3,4] Macroscopically, soft rot is characterized by the softening of wood due to cellulose destruction, which distinguishes it from white rot and brown rot.

Previous insights into the patterns of wood deterioration throughout geological history have mainly been derived from silicified wood remains.[7] Notably, nearly all documented records of fossil fungal wood decay from the Paleozoic and Mesozoic describe white rot, whereas other rot types are rarely documented. Fossilized charcoal represents another beneficial source of information on various paleoecological and paleoenvironmental parameters dating back to the Paleozoic.[8,9] Compared to the slice observation of petrified wood, fossil charcoal provides three-dimensional views of microstructures and can thus serve as an excellent carrier for preserving fungal remains and wood-decay structures. Analysis of archaeological charcoal samples has indicated that fungal infestation and decay features can persist after burning, displaying visible micromorphological details of mycelia and cell wall alterations.[10] However, in pre-Quaternary charcoals, despite the

[1]State Key Laboratory of Palaeobiology and Stratigraphy, Nanjing Institute of Geology and Palaeontology, Chinese Academy of Sciences, 39 East Beijing Road, Nanjing 210008, China
[2]College of Materials Science and Engineering, Nanjing Forestry University, 159 Longpan Road, Nanjing 210037, China
[3]Lead contact
*Correspondence: hzhang@nigpas.ac.cn
https://doi.org/10.1016/j.isci.2024.110000

prevalence of evidence for microbiologically mediated decay, only a few materials have been studied in detail with regard to pre-charring decay by fungi.[11–13] El Atfy et al. (2019) provided the first overview of cell wall alterations associated with pre-charring degradation that have been seen in pre-Quaternary charcoals dating from the Permian to the Paleogene, demonstrating the possibility of recognizing pre-burning microbial activities that are comparable to three major wood rots. Uhl et al. (2020) described various traces of pre-charring decay from the Late Oligocene of Norken and discussed similar plant-microorganism interactions. These studies highlight the considerable potential of fossil charcoal for investigating intricate pre-charring deterioration, which helps further distinguish specific wood-rotting types.

In this study, we collected large amounts of fossil charcoals from the upper Permian strata of Southwest China, Northwest China, and southern Mongolia (see Figures S1 and S2). These charcoals are products of paleo-wildfires during the Late Permian. The details of the charcoals including anatomical structures, reflectance, and stratigraphic distribution have been systematically documented.[14,15] Notably, the charcoals preserved a large amount of evidence for microbiologically mediated decay, including erosions, shoot-like holes, and cavities within cell walls. We identified distinctive decay symptoms corresponding to the three contemporary wood-rot types from these ancient charcoals after comparing them to distinct wood-decay patterns and cell wall modifications in contemporary woods and those recorded from the geological past. These materials, which exhibit a range of wood-decay patterns, provide evidence indicating that all three wood-rotting types existed during the Late Paleozoic. Moreover, they provide insights into the various fungal metabolic strategies that were developed specifically for the destruction of woody tissues during this period.

RESULTS

White rot

White rot can result in various morphological deterioration patterns in wood with different fungal species, wood types, and physiological conditions.[3,4,16] Charcoals from the upper Permian, particularly those collected from the Lengqinggou section, frequently exhibited linear cavities between the walls of neighboring tracheids in transverse views (Figure 1A). The presence of such a division is anomalous because high temperatures homogenize neighboring tracheid walls during charcoalification. Because of the fracture mechanism of charcoal, these structures are more commonly identified in the longitudinal view, which indicates a sequence of distinctive stages. In the early stages of decay, many small cavities with different diameters were formed and aligned between the neighboring tracheid walls (Figure 1B). Similar small cavities at the position of the former middle lamella have been documented in Cretaceous charred wood in Egypt and Germany.[11] In the progressive stage, these cavities fused to form larger cavities, ultimately resulting in the total separation of individual tracheids (Figure 1C). Such advanced signs have been widely documented from fossil woods throughout the geological past,[17–20] which are usually documented as isolations of individual tracheids, i.e., "apposition." These features are generally interpreted as the result of the complete removal of the lignin-rich middle lamella, which is in accordance with the preferential delignification of white rot.[3–5] Unfortunately, these symptoms were not observed in our lab-burned samples, probably because the cultured strain did not show an affinity for lignin.

In addition to preferential delignification, signs of simultaneous rot have been frequently identified in Permian specimens. Simultaneous rot degrades all the main wood components from the cell lumen outwards, with gradual erosion of the surrounding cell wall by the lumen-based hyphae. Morphologically, the rot manifests as pit erosion and lysis grooves in the early stages and ultimately results in progressively thinner cell walls. In Permian charcoals, simultaneous rot is characterized by frequent, rounded notches around the edge of the tracheid lumens in transverse views (Figure 1D); in certain cases, the notches can completely penetrate the walls. More notable features were observed in the longitudinal views, such as crater-like pit erosions at various depths and of different diameters on the smooth surface of the cell walls (Figure 1E), channel-like lysis tracks with sinuous profiles, and several bifurcations (Figure 1F). These decay structures indicate simultaneous deterioration of all cell wall constituents, a capability attributed exclusively to white-rot basidiomycetes.[21] The decay patterns were similar to those observed in the laboratory-charcoalified specimens. In charcoals of white-rotted *Phoebe nanmu*, identical crater-like erosions were observed in ray cells and adjacent tracheids (Figure 1G). Sinuous lysis troughs of fungal hyphae were slenderer than those in Permian charcoal and occasionally extended into holes caused by major pit erosion (Figures 1H and 1I). These pit erosions generally exhibit more advanced stages of decay because they are deeper and almost completely penetrating the walls. However, they could be distinguished from the shot-like holes of brown rot by the irregular outline and remnant tissues in the holes after incomplete enzymolysis (Figures 1H and 1I).

Brown rot

According to previous studies, brown rot is considered difficult to confirm via microstructure examination because the primary structure of cell walls remains unaltered, even in advanced stages of deterioration. The typical symptoms of brown rot are the characteristic wavy appearance of cell walls owing to the lack of strength and shrinkage-induced cubical fractures.[3,4] Subsequent studies suggested that cell walls infected by brown rot fungi would transform into a porous structure,[6,22] and shot-like holes in fossil charcoals are considered evidence for pre-charring brown rot.[11,23] Brown rot fungi are thought to have limited hole-boring abilities; however, their hyphae can directly invade the cell wall via a non-enzymatic oxidation process known as the Fenton reaction.[24] After penetrating cell walls, they secrete enzymes into the secondary wall to rapidly depolymerize the carbohydrate cellulose and hemicelluloses.[4] Brown rot does not cause decorations such as lysis grooves or conspicuous cavities but does result in shot-like holes in cell walls, "wavy" cell walls resulting from loss of rigidity, and cubical fractures resulting from shrinkage.

Analogous shot-like holes were frequently observed in the upper Permian charcoal. These had a smooth edge, were perfectly rounded, and ranged in diameter from 2 to 10 μm (Figures 2A and 2B), which may be related to the variable sizes of the various fungal species. Cross-sectional examination showed that the holes were cone shaped and completely penetrated the cell walls (Figure 2C). In some cases, collapsed

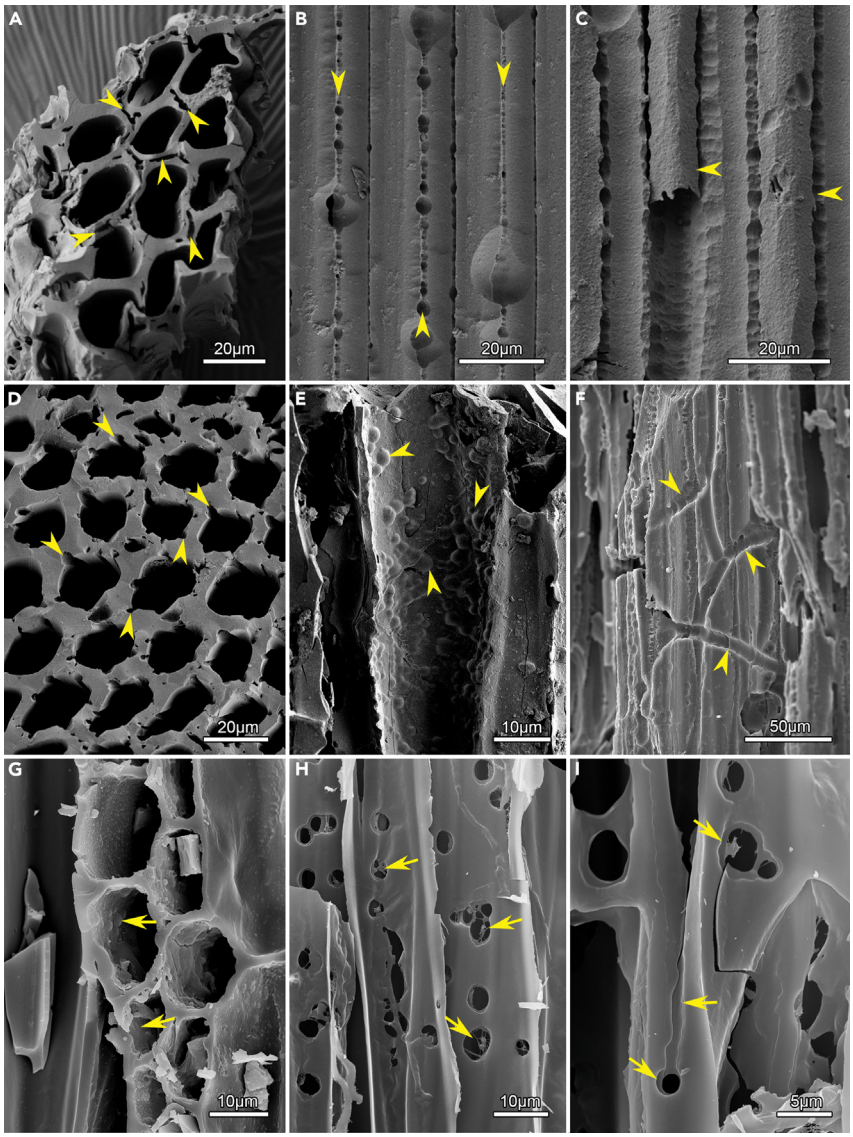

Figure 1. Scanning electron microscope (SEM) images of the charcoals showing symptoms of white rot

(A) Linear cavities between the neighboring tracheid cells (arrows), indicating the dissolution of middle lamellae; Permian charcoal; (B) small cavities aligned between the neighboring tracheid walls (arrows), indicative of the early signs of decay of the middle lamella; Permian charcoal; (C) isolations of individual cells (arrows), indicating a progressing stage of preferential delignification with complete decomposition of the middle lamella; Permian charcoal; (D) frequent pit erosions and lysis tracks (arrows) of fungal hyphae around the edge of tracheid lumens; Permian charcoal; (E) dense pit erosions on the tracheid walls and indicating the simultaneous rot; Permian charcoal; (F) channel-like lysis tracks (arrows) on the tracheid walls, indicating simultaneous rot; Permian charcoal; (G) similar dense pit erosions on the ray cell walls; charcoalified white-rotted *Phoebe nanmu*; (H) severe pit erosions with remnant tissues in holes (shanked arrows); charcoalified white-rotted *Phoebe nanmu*; (I) irregular outlines of boreholes with occasionally lysis tracking them (shanked arrows); charcoalified white-rotted *Phoebe nanmu*.

hyphae were observed in these holes (Figure 2D). In transverse views of the tracheids, the infected cell walls appeared severely distorted, being wavy and compressed (Figure 2E), indicating a loss of mechanical stability due to carbohydrate degradation. In some cases, dense cubic cracks were observed (Figure 2F), which were different from those created during the burning process, and provided hints about the cubical fracture found in brown rot wood resulting from the shrinkage of the cells.[1,3,4] These decay structures were consistent with the aforementioned symptoms of typical brown rot, which were confirmed in our lab-burnt charcoals of brown-rotted wood. The comparable deterioration results in identical shot-like holes with smooth edges of different diameters (Figures 2G and 2H), frequent hyphal penetration (Figure 2I), and the typical wavy appearance of the degraded cell walls in the transverse view (Figure 2J). However, these symptoms were rarer in lab-burned charcoal than in Permian specimens, and cubical fractures were not observed in brown-rotted *Phoebe nanmu*. This discrepancy may be attributable to the different decay stages or the species of infected fungi and host woody plants.

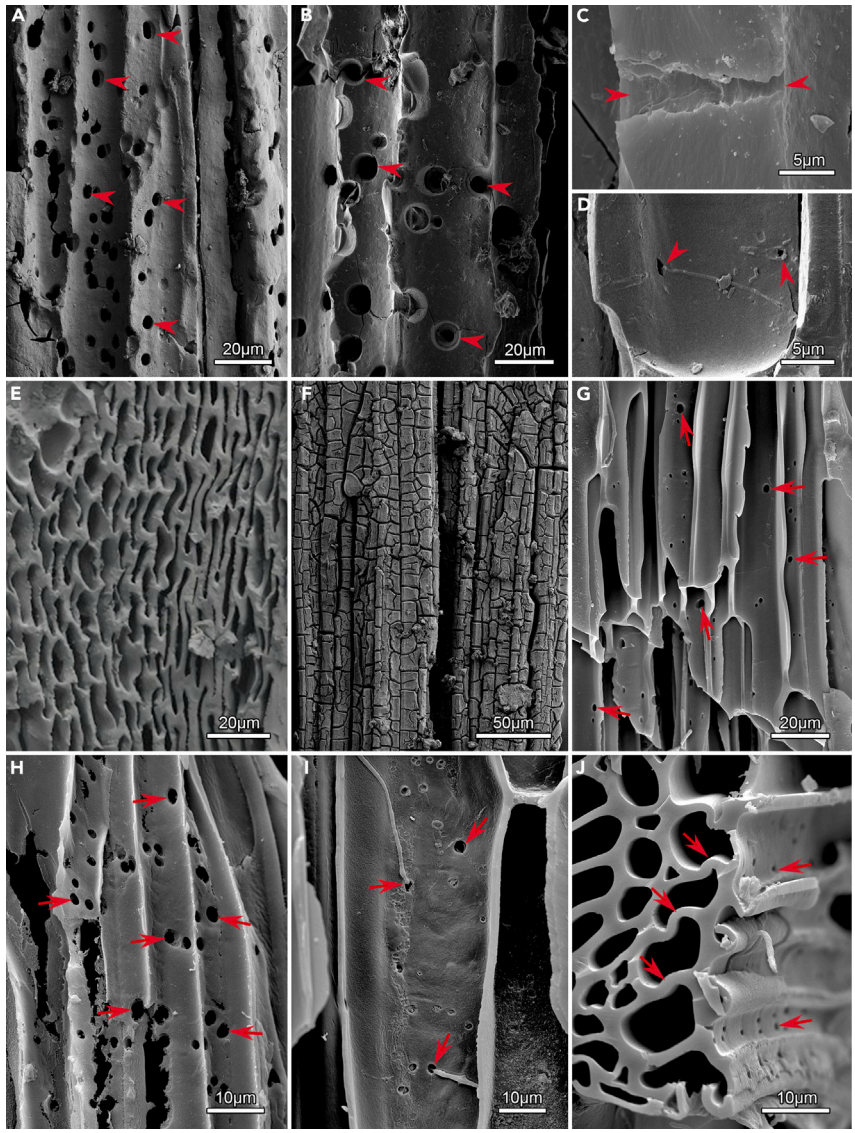

Figure 2. Scanning electron microscope (SEM) images of the charcoals with signs of brown rot

(A and B) Frequent shot-like holes (arrows) of various diameters through the cell walls; Permian charcoals; (C) close-up of a radial cut of the tracheid wall, showing the shot-like hole completely penetrating the wall (arrows); Permian charcoal; (D) a charred fungal hypha penetrating the wall through a shot-like hole (arrows); Permian charcoal; (E) cross-sectional view showing "wavy" cell walls and compressed tracheids, indicative of brown rot; Permian charcoal; (F) tracheids with dense cubic cracks after shrinkage due to drying; Permian charcoal; (G, H) similar shot-like holes (shanked arrows) of various diameters through the cell walls; charcoalified brown-rotted *Phoebe nanmu*; (I) shot-like holes with charred fungal hyphae penetrating through them (shanked arrows); charcoalified brown-rotted *Phoebe nanmu*; (J) cross-sectional view of infected tracheids showing wavy cell walls (shanked arrows); charcoalified brown-rotted *Phoebe nanmu*.

Soft rot

Soft rot is caused by ascomycetes and deuteromycetes, which show a preference for cellulose and hemicellulose and consume a limited amount of lignin.[1,3,4] Microscopically, soft rot generates two morphologically distinct decay patterns: type I (cavity formation) and type II (cell wall erosion).[4] Microfungi of type I have specialized hyphae (~0.5 μm in diameter) to drill in the cell wall and characteristically grow along the microfibrils in the secondary wall.[3,4] In this case, the most diagnostic microscopic traits of type I soft rot are distinctive biconical and cylindrical cavities within the secondary (S2) cell wall layers, which are associated with cellulolytic microfibrillar orientation.[25,26] Type II soft rot is similar to simultaneous white rot and can degrade the entire secondary wall while retaining the middle lamellae. This form of degradation is typically observed in low-lignin hardwoods, particularly in environments with high moisture levels.[6]

The Permian charcoal showed representative characteristics of type I soft rot. In charcoal fragments from the Dalongkou section of Northwest China, dense cavities with conical ends within the S2 cell wall layers were identified at high magnification in the longitudinal sections of

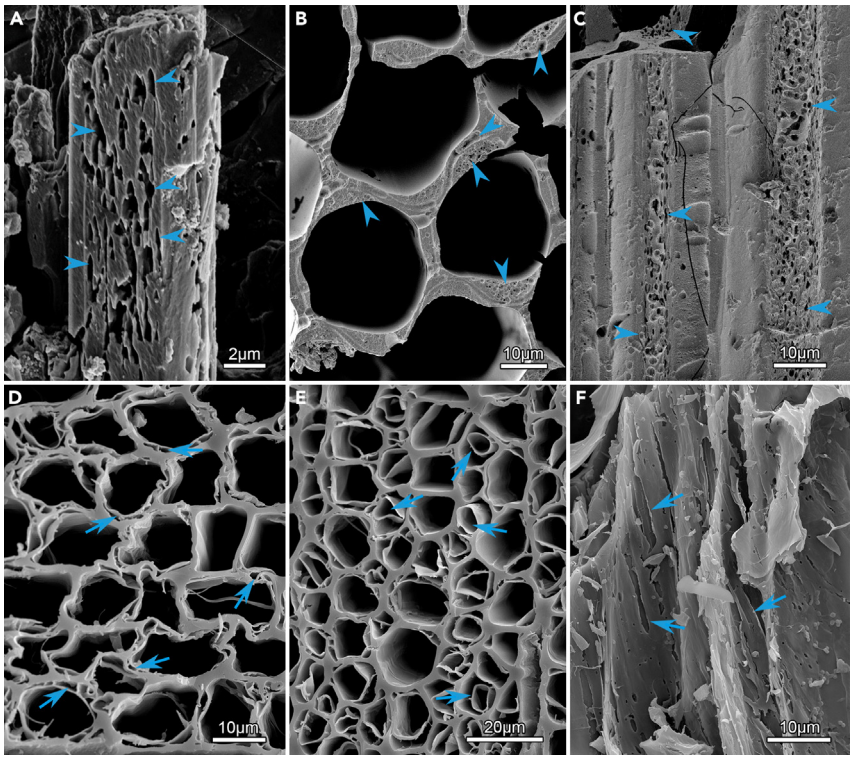

Figure 3. Scanning electron microscope (SEM) images of the charcoals showing signs of soft rot

(A) Close-up of a radial cut of the tracheid wall, highlighting cavities with conically shaped ends within the S2 cell wall layer (arrows), indicative of soft rot; Permian charcoal; (B) cross-sectional view showing abundant cavities and erosions (arrows) within the S2 cell wall layers; Permian charcoal; (C) dense, small, and shallow boreholes (arrows) in the secondary/tertiary cell walls; Permian charcoal; (D) numerous irregular cavities in the S2 cell wall layers with intact middle lamella; charcoalified soft-rotted *Cinnamomum camphora*; (E) rotten tracheids showing degradation of entire S2 cell wall layers, leaving papery S3 layers (shanked arrows); charcoalified soft-rotted *Cinnamomum camphora*; (F) the longitudinal view showing the papery S3 layers that crimp and desquamate; charcoalified soft-rotted *Cinnamomum camphora*.

the cell walls (Figure 3A), which were identical to the descriptions and illustrations provided in previous studies. Similar miniscule cavities inside the S2 cell wall layers were more frequently observed in transverse views of charcoals from the Lengqinggou area of Southwest China, although these cavities exhibited more circular shapes (Figure 3B). Erosion channels caused by proboscis hyphae within the S2 cell wall layers were also observed in the transverse views (Figure 3B). Furthermore, the longitudinal degradation features of the tertiary (S3) cell wall layers could be examined because of the three-dimensional preservation of charcoal. The longitudinal view of the soft-rotted tracheids showed dense small (<1 μm diameter) but shallow boreholes in the secondary and/or tertiary cell walls (Figure 3C). These were reminiscent of the specialized hyphae of soft rot that bore into the S2 cell wall layers from the tracheid lumens. Such decay structures were even more common in Permian charcoals from Southwest China.

In the lab-burned charcoals, similar soft rot deterioration patterns were frequently observed, particularly in transverse views, where they appeared as numerous circulars, irregular to crescentic cavities in the S2 cell wall layers, whereas areas of the middle lamella remained intact (Figure 3D). These cavities were much larger than those observed in Permian charcoal, which is likely related to different fungal species or advanced stages of decay. Some rotten tracheids showed degradation of entire S2 cell wall layers, resulting in papery S3 layers (Figure 3E). This was also observed in the longitudinal views, where the papery S3 layers were generally crimped and desquamated (Figure 3F). Therefore, the small and shallow boreholes on the cell walls, which may be signs of early-stage decay, were rarely observed in the laboratory soft-rotted charcoal.

DISCUSSION

Since the emergence of forests, the accumulation and decomposition of woody biomass have been in dynamic equilibrium in natural ecosystems, which may have influenced coal burial in geological history.[27,28] Initially, it was thought that the substantial accumulation of organic carbon (C_{org}) during the Permo-Carboniferous occurred partly because the fungi capable of effectively breaking down lignin had not evolved or diversified.[29] Similarly, molecular clock analyses have suggested that the origin of lignin degradation may have coincided with an abrupt decline in the rate of C_{org} burial at the end of the Carboniferous.[27] However, these hypotheses were contradicted by later investigations, which showed that lignin-degrading fungi may have been present before the Carboniferous and that a large proportion of Carboniferous

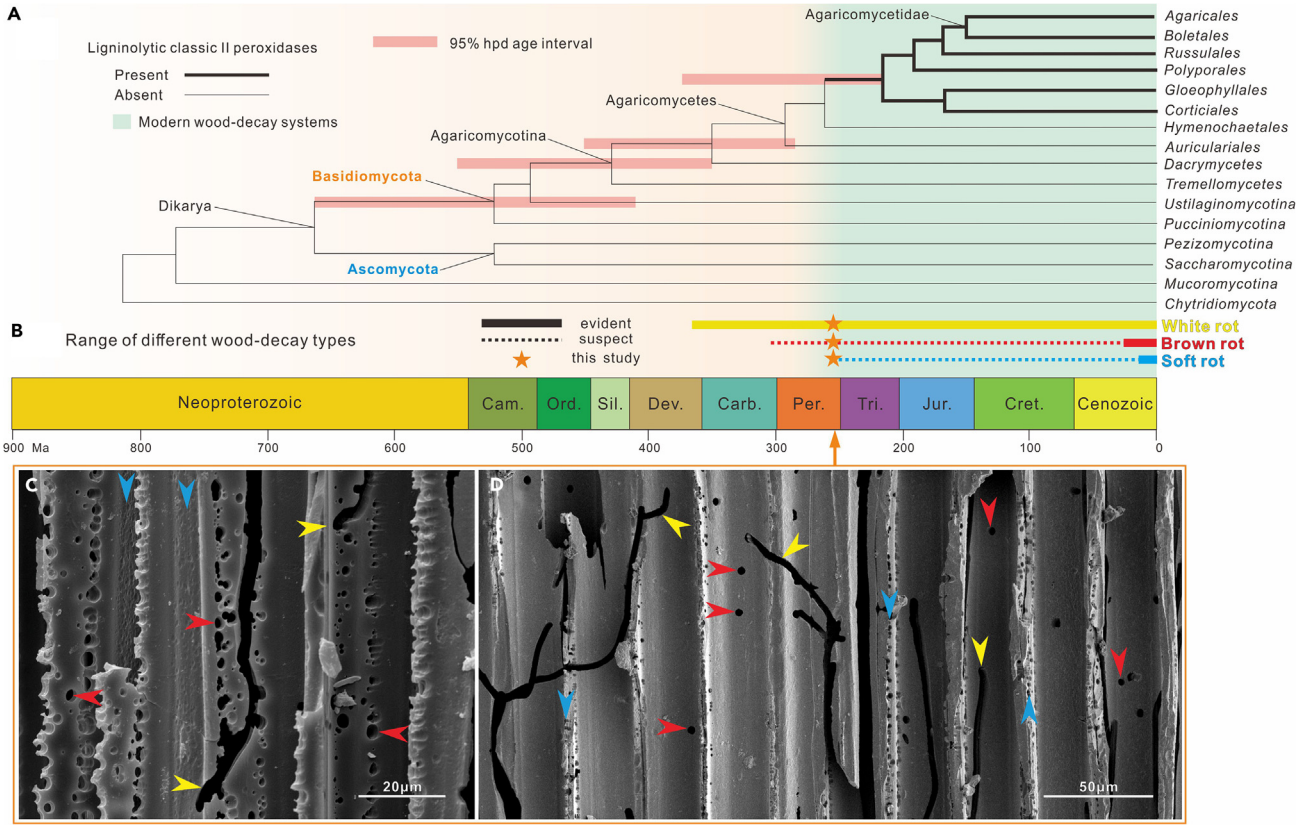

Figure 4. The compilation of potential origins for different wood-decay types based on phylogenomic and fossil data in geological history

(A) Phylogenomic data showing the evolution of major fungal groups, modified from Floudas et al. (2012)[27] and Hibbett et al. (2016)[28]; (B) the range of rot types based on documented fossil evidence, including evident and suspected records; (C and D) the co-occurrence of signs of white rot (yellow arrows), brown rot (red arrows), and small cavities or shallow holes in secondary cell walls that are indicative of soft rot (blue arrows) on the same specimen.

coals were dominated by unlignified plant tissues.[28,30] Nevertheless, phylogenomic investigations have revealed that the ability to decompose cellulose and hemicellulose dates back to the Cambrian Period; however, ligninolytic systems comparable to modern white rot emerged more recently within Agaricomycetes, possibly during the Permo-Carboniferous[28] (Figure 4A).

Nonetheless, direct fossil evidence of plant-fungus interactions is scarce in the geological record, particularly that representing the current range of recognized patterns of wood rot (Figure 4B). The earliest record of white rot, as well as the oldest example of wood decay caused by fungi, was documented in progymnosperm woods from the Upper Devonian in North America, which exhibited an altered structure with extensive cell wall lysis and distinct erosion troughs, with the occurrence of septate hyphae resembling those of basidiomycetes and ascomycetes.[7] Additionally, similar evidence of white rot, as well as white pocket rot, has been frequently documented from petrified woods throughout geological history.[25,31–33] However, it is intriguing to note that white rot is the only type of rot that has been definitively identified in fossil records of fungal wood deterioration dating back to the Paleozoic and Mesozoic. In contrast, the first geological records of brown rot date back to the late Oligocene, based on charcoal evidence showing shot-like holes and "wavy" cell walls.[11] Similar boreholes in charcoals have been reported from the Late Carboniferous[34]; however, this evidence is insufficient to assign them to symptoms of brown rot because white-rot fungi can also penetrate cell walls. Soft rot can be traced back to the early Miocene,[31] although plausible soft rot decay of Antarctic woods from the Eocene has been identified[35] and some granular alterations with suspected morphological similarities to soft rot symptoms have been observed in fossil wood from the upper Permian.[25]

In present-day ecosystems, white-rot fungi generally colonize hardwood, whereas brown-rot fungi are more likely to infect softwood.[36,37] Considering the absence of hardwood and the prevalence of white rot in softwood during the Paleozoic, it appears that fungal preferences for decayed hosts changed significantly with floral evolution. However, from a different perspective, spore-bearing plants have been shown to contain an unusually high lignin content compared with the seed plants,[29] and hardwoods in broad terms contain different lignin monomers and lower lignin content than softwoods.[4,6] In this context, it is reasonable to assume that white rot was the earliest and most prevalent wood-decay type in the Paleozoic, as it is the only decay type that effectively degrades lignin. However, the ancient white rot could be different from the current form because of the difference in lignin monomers in spore-bearing plants and modern hardwoods. This interpretation aligns with the molecular data, which indicated that ligninolytic systems similar to modern white rot appeared during the Late Paleozoic. It is likely that

brown rot and soft rot, which mainly metabolize cellulose and hemicelluloses, were specialized and adaptive strategies for wood-decay fungi after the prevalence of seed plants during the Late Paleozoic. In the decay process, brown rot combines non-enzymatic and enzymatic degradation mechanisms, rapidly colonizes an unexploited substrate, and more effectively degrades cellulose and hemicellulose, even when the hyphae and the wood cell wall are not in close proximity to each other.[4] Soft rot exhibits greater adaptability to occupy ecological niches under extreme conditions, including aquatic environments, which are unfavorable for other types of decay.

Phylogenomic analyses indicate that major fungal groups were already represented by the end of the Paleozoic,[27,28] including most families of Basidiomycetes, which can cause white rot and brown rot (Figure 4A). Although molecular data and plausible evidence suggest that fungi have evolved the capacity to decay different cell wall components of plants via multiple decay strategies over the Late Paleozoic,[25,27,28] it is nonetheless remarkable to observe the direct preservation of all wood-rot patterns within the contemporaneous charcoal assemblages from the Permian. This evidence suggests that the wood-decay strategies in the preferred substrate and adaptation to extreme environments had already begun to diverge by the Late Paleozoic. The lack of brown rot and soft rot in fossil records may not be attributable to their absence during this period but to the variable nature of the decay and the resultant wood texture. For instance, brown-rotted wood does not preserve and fossilize easily owing to its delicate and brittle nature, and soft-rotted wood typically appears in restricted environments with very wet or dry conditions, making it less well represented than other rot types and less likely to petrify or encounter wildfires.

Notably, some Permian specimens from Southwest China exhibited characteristics of two or three rot patterns, including shot-like holes that completely passed through the cell walls, small boreholes penetrating into the secondary walls, and sinuous erosion troughs cutting through the entire walls (Figures 4C and 4D). This mirrors the conditions in present-day ecosystems, where multiple fungi infect and colonize the same wood simultaneously or successively.[38,39] The competition and interaction between different fungi can accelerate wood degradation, facilitating rapid colonization of unexploited or easily degradable substrates, and can lead to thorough wood degradation based on complementary enzymatic capacities for different substrates. Another explanation for the co-occurrence of multiple rot patterns is that some fungi can switch between different patterns of decay under certain environmental conditions. For instance, white-rot fungi have been documented to cause facultative soft rot in wood from the Miocene,[31] and some modern fungi have been found using such decay strategies to circumvent plant defenses.[40] In our laboratory, *Phoebe nanmu* inoculated with *Trametes versicolor*, a white-rot fungus, occasionally displayed signs typically associated with brown rot, such as similar shot-like holes and wavy cell walls. This is reminiscent of a genomic analysis, which suggests that the white-rot and brown-rot patterns of wood degradation are more of a continuum than a dichotomy,[41] although this is beyond the scope of this study. Additionally, different rot types sometimes represent strategies to adapt to diverse environmental conditions, such as the typical occurrence of soft rot under very wet/dry or low-oxygen conditions.[1] The presence of typical soft rot and the rare occurrence of white rot and brown rot in Northwest China probably reflect the challenging environmental conditions for the growth of most fungi. In contrast, the co-occurrence of multiple decay symptoms may indicate changes in certain environmental conditions such as the transport of pre-charred wood into aquatic environments. Among the three charcoal-bearing areas, the largest amount of charcoal exhibiting signs of biodeterioration was observed in the Lengqinggou section of Southwest China, which was a swamp rainforest during the Late Permian. This corresponds to current conditions, in which warm temperatures and high moisture levels are favorable for fungal growth. Moreover, the abundant plant substrates and diversity of local environmental conditions enabled different wood-decay fungi to develop all of the aforementioned strategies. These cases indicate a high degree of ecological complexity between diverse wood-decay strategies and flourishing plant communities in Late Paleozoic terrestrial ecosystems.

Limitations of the study

Current wood-rotting fungi show a significant preference for hosts such as hardwood and softwood; thus it is challenging to locate a counterpart study for the current situation based on charcoal fragments that are exclusively derived from gymnosperms. Since the charcoal specimens are composed entirely of carbon only, Fourier transform infrared spectroscopy cannot be used to identify the consumed components that help distinguish between different types of wood rot. The present study mainly provides morphological evidence of multiple wood-rotting strategies during the Late Paleozoic; thus, further studies are needed to fully understand the decay process and the evolution of these strategies.

STAR★METHODS

Detailed methods are provided in the online version of this paper and include the following:

- KEY RESOURCES TABLE
- RESOURCE AVAILABILITY
  - Lead contact
  - Materials availability
  - Data and code availability
- EXPERIMENTAL MODEL AND STUDY PARTICIPANT DETAILS
  - Geological context and the fossil materials
  - Modern decay wood with different rot patterns
- METHOD DETAILS
  - Extraction of the permian charcoals

- Decay experiments of modern woods
- Charcoalification of modern decay woods
- QUANTIFICATION AND STATISTICAL ANALYSIS

SUPPLEMENTAL INFORMATION

Supplemental information can be found online at https://doi.org/10.1016/j.isci.2024.110000.

ACKNOWLEDGMENTS

This work was funded by the National Natural Science Foundation of China (42293280) and the Jiangsu Innovation Support Plan for International Science and Technology Cooperation Programme (BZ2023068).

We deeply appreciate professors S. Z. Shen and Z. Feng for the help in the field. We also acknowledge X.S. Zhang and C.Z. Wang for the experimental assistance.

We thank the editor for the editorial handling of this manuscript and the reviewers for their constructive suggestions to improve it.

AUTHOR CONTRIBUTIONS

Conceptualization, Y.C. and H.Z.; methodology, Y.C.; investigation, Y.C. and B.P.; resources, H.Z. and B.P.; writing – original draft, Y.C.; writing – review & editing, Y.C. and H.Z.; visualization, Y.C.; supervision, H.Z.; funding acquisition, H.Z.

DECLARATION OF INTERESTS

The authors declare no competing interests.

Received: September 20, 2023
Revised: March 19, 2024
Accepted: May 14, 2024
Published: May 15, 2024

REFERENCES

1. Schmidt, O. (2006). Wood and Tree Fungi Biology, Damage, Protection, and Use. (Springer-Verlag), pp. 1–334. https://doi.org/10.1007/3-540-32139-X.
2. Singh, R., Upadhyay, S.K., Rani, A., Kumar, P., Kumar, A., and Singh, C. (2018). Lignin Biodegradation in Nature and Significance. Vegetos *31*, 39. https://doi.org/10.5958/2229-4473.2018.00091.5.
3. Schwarze, F.W. (2007). Wood decay under the microscope. Fungal Biol. Rev. *21*, 133–170. https://doi.org/10.1016/j.fbr.2007.09.001.
4. Daniel, G. (2003). Microview of wood under degradation by bacteria and fungi. In Wood Deterioration and Preservation, B. Goodell, D.D. Nicholas, and T.P. Schultz, eds. (ACS Symposium), pp. 34–72.
5. Schwarze, F.W.M.R., Engels, J., and Mattheck, C. (2000). Fungal Strategies of Wood Decay in Trees (Springer-Verlag), pp. 1–185. https://doi.org/10.1007/978-3-642-57302-6.
6. Daniel, G. (2016). Fungal Degradation of Wood Cell Walls. In Secondary Xylem Biology: Origins, Functions, and Applications, Y.S. Kim, R. Funada, and A.P. Singh, eds. (Academic Press), pp. 131–167. https://doi.org/10.1016/b978-0-12-802185-9.00008-5.
7. Stubblefield, S.P., Taylor, T.N., and Beck, C.B. (1985). Studies of Paleozoic fungi. IV. Wooddecaying fungi in Callixylon newberryi from the Upper Devonian. Am. J. Bot. *72*, 1765–1774. https://doi.org/10.2307/2443734.
8. Scott, A.C. (2000). The Pre-Quaternary history of fire. Palaeogeogr. Palaeoclimatol. Palaeoecol. *164*, 281–329.
9. Scott, A.C., and Damblon, F. (2010). Charcoal: Taphonomy and significance in geology, botany and archaeology. Palaeogeogr. Palaeoclimatol. Palaeoecol. *291*, 1–10.
10. Moskal-del Hoyo, M., Wachowiak, M., and Blanchette, R.A. (2010). Preservation of fungi in archaeological charcoal. J. Archaeol. Sci. *37*, 2106–2116. https://doi.org/10.1016/j.jas.2010.02.007.
11. El Atfy, H., Havlik, P., Krüger, P.S., Manfroi, J., Jasper, A., and Uhl, D. (2019). Pre-Quaternary wood decay 'caught in the act' by fire – examples of plant-microbeinteractions preserved in charcoal from clastic sediments. Hist. Biol. *31*, 952–961.
12. Uhl, D., Wuttke, M., and Jasper, A. (2020). Woody charcoal with traces of pre-charring decay from the Late Oligocene (Chattian) of Norken (Westerwald, Rhineland-Palatinate, W Germany). Acta Palaeobot. *60*, 43–50. https://doi.org/10.35535/acpa-2020-0002.
13. Uhl, D., Jasper, A., Solórzano Kraemer, M., and Wilde, V. (2019). Charred biota from an Early Cretaceous fissure fill in W-Germany and their palaeoenvironmental implications. NJGPA *293*, 83–105. https://doi.org/10.1127/njgpa/2019/0833.
14. Cai, Y.F., Zhang, H., Feng, Z., and Shen, S.Z. (2021). Intensive Wildfire Associated With Volcanism Promoted the Vegetation Changeover in Southwest China During the Permian–Triassic Transition. Front. Earth Sci. *9*. https://doi.org/10.3389/feart.2021.615841.
15. Cai, Y.F., Zhang, H., Cao, C.Q., Zheng, Q.F., Jin, C.F., and Shen, S.Z. (2021). Wildfires and deforestation during the Permian–Triassic transition in the southern Junggar Basin, Northwest China. Earth Sci. Rev. *218*, 103670. https://doi.org/10.1016/j.earscirev.2021.103670.
16. Blanchette, R.A., Nilsson, T., Daniel, G., and Abad, A. (1990). Biological degradation of wood. In Archaeological Wood Properties, Chemistry, and Preservation, R.M. Rowell and R.J. Barbour, eds. (American Chemical Society), pp. 141–174.
17. Weaver, L., McLoughlin, S., and Drinnan, A.N. (1997). Fossil woods from the Upper Permian Bainmedart Coal Measures, northern Prince Charles Mountains, East Antarctica. J. Australian Geol. Geophys. *16*, 655–676.
18. Feng, Z., Wei, H.B., Wang, C.L., Chen, Y.X., Shen, J.J., and Yang, J.Y. (2015). Wood decay of Xenoxylon yunnanensis Feng sp. nov. from the Middle Jurassic of Yunnan Province, China. Palaeogeogr. Palaeoclimatol. Palaeoecol. *433*, 60–70. https://doi.org/10.1016/j.palaeo.2015.05.021.
19. Wan, M., Yang, W., Liu, L., and Wang, J. (2016). Plant-arthropod and plant-fungus interactions in late Permian gymnospermous woods from the Bogda Mountains, Xinjiang, northwestern China. Rev. Palaeobot. Palynol. *235*, 120–128. https://doi.org/10.1016/j.revpalbo.2016.10.003.
20. Greppi, C.D., Alvarez, B., Pujana, R.R., Ibiricu, L.M., and Casal, G.A. (2022). Fossil woods with evidence of wood-decay by fungi from the Upper Cretaceous (Bajo Barreal Formation) of central Argentinean Patagonia. Cretac. Res. *136*, 105229. https://doi.org/10.1016/j.cretres.2022.105229.
21. Otjen, L., and Blanchette, R.A. (1986). A discussion of microstructural changes in wood during decomposition by white rot

basidiomycetes. Can. J. Bot. *64*, 905–911. https://doi.org/10.1139/b86-121.
22. Bari, E., Daniel, G., Yilgor, N., Kim, J.S., Tajick-Ghanbary, M.A., Singh, A.P., and Ribera, J. (2020). Comparison of the Decay Behavior of Two White-Rot Fungi in Relation to Wood Type and Exposure Conditions. Microorganisms *8*, 1931. https://doi.org/10.3390/microorganisms8121931.
23. Schweingruber, F.H., Börner, A., and Schulze, E.D. (2006). Atlas of Woody Plant Stems Evolution, Structure, and Environmental Modifications (Springer-Verlag), pp. 1–229. https://doi.org/10.1007/3-540-32525-5.
24. Rättö, M., Ritschkoff, A.-C., and Viikari, L. (1997). The effect of oxidative pretreatment on cellulose degradation by Poria placenta and Trichoderma reesei cellulases. Appl. Microbiol. Biotechnol. *48*, 53–57. https://doi.org/10.1007/s002530051014.
25. Harper, C.J., Decombeix, A.-L., Taylor, E.L., Taylor, T.N., and Krings, M. (2017). Fungal decay in Permian Glossopteridalean stem and root wood from Antarctica. IAWA J. *38*, 29–48. https://doi.org/10.1163/22941932-20170155.
26. Pujana, R.R., Massini, J.L.G., Brizuela, R.R., and Burrieza, H.P. (2009). Evidence of fungal activity in silicified gymnosperm wood from the Eocene of southern Patagonia (Argentina). Geobios *42*, 639–647. https://doi.org/10.1016/j.geobios.2009.05.001.
27. Floudas, D., Binder, M., Riley, R., Barry, K., Blanchette, R.A., Henrissat, B., Martínez, A.T., Otillar, R., Spatafora, J.W., Yadav, J.S., et al. (2012). The Paleozoic Origin of Enzymatic Lignin Decomposition Reconstructed from 31 Fungal Genomes. Science *336*, 1715–1719.
28. Hibbett, D., Blanchette, R., Kenrick, P., and Mills, B. (2016). Climate, decay, and the death of the coal forests. Curr. Biol. *26*, R563–R567. https://doi.org/10.1016/j.cub.2016.01.014.
29. Robinson, J.M. (1990). Lignin, land plants, and fungi: biological evolution affecting Phanerozoic oxygen balance. Geology *18*, 607–610.
30. Nelsen, M.P., DiMichele, W.A., Peters, S.E., and Boyce, C.K. (2016). Delayed fungal evolution did not cause the Paleozoic peak in coal production. Proc. Natl. Acad. Sci. USA *113*, 2442–2447. https://doi.org/10.1073/pnas.1517943113.
31. Greppi, C.D., García Massini, J.L., Pujana, R.R., and Marenssi, S.A. (2018). Fungal wood-decay strategies in Nothofagaceae woods from Miocene deposits in southern Patagonia, Argentina. Alcheringa *42*, 427–440. https://doi.org/10.1080/03115518.2018.1471736.
32. Philippe, M., McLoughlin, S., Strullu-Derrien, C., Bamford, M., Kiel, S., Nel, A., and Thévenard, F. (2022). Life in the woods: Taphonomic evolution of a diverse saproxylic community within fossil woods from Upper Cretaceous submarine mass flow deposits (Mzamba Formation, southeast Africa). Gondwana Res. *109*, 113–133. https://doi.org/10.1016/j.gr.2022.04.008.
33. Biswas, A., Bera, M., Khan, M.A., Spicer, R.A., Spicer, T.E.V., Acharya, K., and Bera, S. (2020). Evidence of fungal decay in petrified legume wood from the Neogene of the Bengal Basin, India. Fungal Biol. *124*, 958–968. https://doi.org/10.1016/j.funbio.2020.08.003.
34. Uhl, D., and Jasper, A. (2020). Wildfire during deposition of the "Illinger Flözzone" (Heusweiler-Formation, "Stephanian B". Paleobiodivers. Paleoenviron. *101*, 9–18. https://doi.org/10.1007/s12549-020-00443-2.
35. Cantrill, D.J., and Poole, I. (2005). A new EoceneAraucariafrom Seymour Island, Antarctica: evidence from growth form and bark morphology. Alcheringa *29*, 341–350. https://doi.org/10.1080/03115510508619310.
36. Purahong, W., Wubet, T., Krüger, D., and Buscot, F. (2018). Molecular evidence strongly supports deadwood-inhabiting fungi exhibiting unexpected tree species preferences in temperate forests. ISME J. *12*, 289–295. https://doi.org/10.1038/ismej.2017.177.
37. Rayner, A.D.M., and Boddy, L. (1988). Fungal Decomposition of Wood: Its Biology and Ecology (Wiley), pp. 647–648.
38. Stokland, J.N., Siitonen, J., and Jonsson, B.G. (2012). Biodiversity in Dead Wood (Cambridge University Press), pp. 1–509. https://doi.org/10.1017/CBO9781139025843.
39. Rajala, T., Tuomivirta, T., Pennanen, T., and Mäkipää, R. (2015). Habitat models of wood-inhabiting fungi along a decay gradient of Norway spruce logs. Fungal Ecol. *18*, 48–55. https://doi.org/10.1016/j.funeco.2015.08.007.
40. Schwarze, F.W.M.R., and Fink, S. (1998). Host and cell type affect the mode of degradation by Meripilus giganteus. New Phytol. *139*, 721–731. https://doi.org/10.1046/j.1469-8137.1998.00238.x.
41. Riley, R., Salamov, A.A., Brown, D.W., Nagy, L.G., Floudas, D., Held, B.W., Levasseur, A., Lombard, V., Morin, E., Otillar, R., et al. (2014). Extensive sampling of basidiomycete genomes demonstrates inadequacy of the white-rot/brown-rot paradigm for wood decay fungi. Proc. Natl. Acad. Sci. USA *111*, 9923–9928. https://doi.org/10.1073/pnas.1400592111.
42. Zhao, X.H., Mo, Z.G., Zhang, S.Z., and Yao, Z.Q. (1980). Late Permian flora in Western Guizhou and Eastern Yunnan. In Stratigraphy and palaeontology of upper Permian coal-bearing formation in Western Guizhou and Eastern Yunnan (Science Press), pp. 1–69.
43. Shen, S.Z., Crowley, J.L., Wang, Y., Bowring, S.A., Erwin, D.H., Sadler, P.M., Cao, C.Q., Rothman, D.H., Henderson, C.M., Ramezani, J., et al. (2011). Calibrating the end-Permian mass extinction. Science *334*, 1367–1372.
44. Zhang, H., Cao, C.Q., Liu, X.L., Mu, L., Zheng, Q.F., Liu, F., Xiang, L., Liu, L.J., and Shen, S.Z. (2016). The terrestrial end-Permian mass extinction in South China. Palaeogeogr. Palaeoclimatol. Palaeoecol. *448*, 108–124.
45. Jiao, S., Zhang, H., Cai, Y., Chen, J., Feng, Z., and Shen, S. (2023). Collapse of tropical rainforest ecosystems caused by high-temperature wildfires during the end-Permian mass extinction. Earth Planet Sci. Lett. *614*, 118193.
46. Cai, Y.F., Zhang, H., Feng, Z., Cao, C.Q., and Zheng, Q.F. (2019). A *Germaropteris*-dominated flora from the upper Permian of the Dalongkou section, Xinjiang, Northwest China, and its paleoclimatic and paleoenvironmental implications. Rev. Palaeobot. Palynol. *266*, 61–71.
47. Johnson, C.L., Amory, J.A., Zinniker, D., Lamb, M.A., Graham, S.A., Affolter, M., and Badarch, G. (2008). Sedimentary response to arc-continent collision, Permian, southern Mongolia. In Formation and Applications of the Sedimentary Record in Arc Collision Zones, *436*, A. Draut, P.D. Clift, and D.W. Scholl, eds. (Geol. Soc. Am. Spe. Papvol.), pp. 363–390.
48. Cai, Y.F., Zhang, H., Feng, Z., Gou, X.D., Byambajav, U., Zhang, Y.C., Yuan, D.X., Qie, W.K., Xu, H.P., Cao, C.Q., et al. (2022). A new conifer stem, *Ductoagathoxylon tsaaganensis*, from the upper Permian of the South Gobi Basin, Mongolia and its paleoclimatic and paleoecological implications. Rev. Palaeobot. Palynol. *304*, 104719.
49. Cai, Y.F., Zhang, H., Feng, Z., Zhang, Y.C., Yuan, D.X., Xu, H.P., Byambajav, U., Yarinpuil, A., and Shen, S.Z. (2023). *Secrospiroxylon tolgoyensis* gen. nov. et sp. nov., a unique coniferous stem from the uppermost Permian of the South Gobi Basin, Mongolia, and its palaeoclimatic, palaeoecophysiological, and palaeoecological implications. Palaeontographica Abteilung B *305*, 93–119.
50. Belcher, C., Collinson, M., and Scott, A. (2005). Constraints on the thermal energy released from the Chicxulub impactor: new evidence from multi-method charcoal analysis. J. Geol. Soc. *162*, 591–602. https://doi.org/10.1144/0016-764904-104.
51. Scott, A.C. (2010). Charcoal recognition, taphonomy and uses in palaeoenvironmental analysis. Palaeogeogr. Palaeoclimatol. Palaeoecol. *291*, 11–39. https://doi.org/10.1016/j.palaeo.2009.12.012.
52. K., J.I.S. (2004). Test methods for determining the effectiveness of wood preservatives and their performance requirements (Japanese Standards Association), p. 1571. https://cir.nii.ac.jp/crid/1571980075899798400#citations_container.

STAR★METHODS

KEY RESOURCES TABLE

REAGENT or RESOURCE	SOURCE	IDENTIFIER
Bacterial and virus strains		
Trametes versicolor	Research Institute for Sustainable Humanosphere in Kyoto University	N/A
Fomitopsis palustris	Research Institute for Sustainable Humanosphere in Kyoto University	N/A
Biological samples		
Phoebe nanmu	Wood collection of Nanjing Forestry University	NFUw77149
Cinnamomum camphora	Wood collection of Nanjing Forestry University	NFUw79617
Critical commercial assays		
Hydrochloric Acid	JiuYi Reagent	81013
Hydrofluoric Acid	Jiuyi Reagent	81016
Deposited data		
Samples of fossil charcoals	This paper, Nanjing Institute of Geology and Palaeontology, CAS	DLK-16/LQG-17/TT-18
Samples of charred decay-wood	This paper, Nanjing Institute of Geology and Palaeontology, CAS	WR-23/BR-23/SR-23
SEM photographs of decay- symptom on the charcoals	This paper	N/A
Experimental models: Organisms/strains		
Japanese Fungal Inoculation Standard	Japanese Standards Association	JIS K. 1571: 2004
Standard process of charcoal extraction	This paper, Nanjing Institute of Geology and Palaeontology, CAS	N/A
Software and algorithms		
CorelDRAW Graphics Suite 2023	Corel Corporation	https://www.coreldraw.com/cn/#
Adobe Photoshop	Adobe Inc.	https://www.adobe.com/hk_zh/products/photoshop.html
Other		
Quantitative data and anatomical structures of the Permian charcoals	Cai et al. (2021a, 2021b)[14,15]; This paper	https://www.sciencedirect.com/science/article/pii/S0012825221001719 https://www.frontiersin.org/articles/10.3389/feart.2021.615841/full

RESOURCE AVAILABILITY

Lead contact

Further requests for the r resources should be directed to the lead contact, Hua Zhang (hzhang@nigpas.ac.cn).

Materials availability

Fossil charcoal materials were deposited at the Nanjing Institute of Geology and Palaeontology, Chinese Academy of Sciences.

Data and code availability

- All data reported in this paper will be shared by the lead contact upon request.
- This paper does not report original code.
- Any additional information required to reanalyze the data reported in this paper is available from the lead contact upon request.

EXPERIMENTAL MODEL AND STUDY PARTICIPANT DETAILS

Geological context and the fossil materials

The fossil materials examined in this study were collected from the Permian–Triassic transitional strata of the Lengqinggou Section in Southwest China, the Dalongkou Section in Northwest China, and the Tsaagan Tolgoy Section in southern Mongolia (see Figure S1).

The Lengqinggou Section (104° 20′ 13″ E; 27° 15′ 46″ N) is in Hezhang County of Bijie City, western Guizhou Province. During the Permian, this area was situated near the equatorial zone and possessed the distinctive Cathaysian *Gigantopteris* flora of tropical peatlands.[42] Thousands of mesoscopic to macroscopic charcoal particles have been collected from the upper Permian Xuanwei Formation, which were regarded as direct evidence of paleo-wildfires induced by drought climate[43,44] and local volcanisms.[14,45] Detailed description of the charcoal anatomical structures and the quantification of charcoal abundance have been documented in Cai et al. (2021a).[14] On these charcoals, wood-decay structures are commonly observed and diverse.

The Dalongkou Section (88° 46′ 48″ E; 43° 49′ 12″ N) is in the Xinjiang Uygur Autonomous Region in Northwest China. This area was within the Kazakhstan–Junggar plate in the northern mid-latitudes during the Permian–Triassic, and experienced a floral change from Angara to sub-Angara due to the drought climate.[46] Charcoal fragments were common and interpreted as the product of frequent paleo-wildfires in this section. Detailed sizes, anatomical structures, and the distribution of the charcoals have been described in Cai et al. (2021b).[15] Among these charcoals, wood-decay structures and fungal remains are rarely observed but crucial.

The Tsaagan Tolgoy Section (105°27′26.3″ E; 42°52′52.8″ N) is situated in the South Gobi Basin, south-central Mongolia.[47] This area was situated in the eastern margin of the mid-latitude Angara and developed the typical Angara Flora during the Late Permian. Evidence from fossil woods indicated a seasonal, temperate, and wet climate.[48,49] Similarly, charcoals were common in this sequence. The detailed analysis of these charcoals is prepared for an unpublished manuscript. Fungal remains and wood-decay structures are frequently observed in both charcoals and fossil woods.

Modern decay wood with different rot patterns

In order to compare the decay traits of Permian charcoals with contemporary rot patterns, three distinct groups of rotten wood, each decayed by specific fungal strains, were obtained from Nanjing Forestry University. The experiments of wood decay were previously conducted in the Research Institute for Sustainable Humanosphere in Kyoto University, with standard wood-decay fungal strains (*Trametes versicolor*, *Fomitopsis palustris*) from the Institute and wood samples (*Phoebe nanmu*, NFUw77149; *Cinnamomum camphora*, NFUw79617) from the Wood collection of Nanjing Forestry University. The charcoalification of the rotten wood samples and further SEM observation and comparison based on morphological similarities were conducted in Nanjing Institute of Geology and Palaeontology, Chinese Academy of Sciences.

METHOD DETAILS

Extraction of the permian charcoals

The primary procedures of charcoal extraction are revised from Belcher et al. (2005)[50] and Scott (2010).[51] The charcoal fragments were extracted by acid maceration as follows (see Figure S3): bulk samples were broken up and immersed in hydrochloric acid (10%) for 24 h to remove carbonates; after rinsing, they were digested with concentrated hydrofluoric acid (40%) for 1 week to remove silicates. The remaining matrix was rinsed again, filtrated using a 30-μm sieve, and boiled in concentrated hydrochloric acid for 20 min to prevent the precipitation of calcium fluoride. The product was then rinsed again, drained, and dried at approximately 70°C in a laboratory oven. Subsequently, charcoal fragments showing features such as black color and silky luster were selected from the acid-treated residue under an Olympus SZX7 stereomicroscope using preparation needles, lancets, script liners, and tweezers. The well-preserved charcoal pieces were subsequently mounted on standard stubs with adhesive tabs for morpho-anatomical observation under a LEO1530VP scanning electron microscope (SEM) after applying a gold coating.

Decay experiments of modern woods

The preparation for modern decay woods followed the Japanese Fungal Inoculation Standard of JIS K. 1571: 2004.[52] Three groups of wood samples were prepared and each consisted of several wooden blocks with dimensions of 20 mm × 20 mm × 10 mm. Due to the preferences of modern decaying fungi, different wood species were used. After disinfection, two groups consisting of *Phoebe nanmu* were inoculated with white rot fungi *Trametes versicolor* and brown rot fungi *Fomitopsis palustris*. Then they were sealed in the glass bottles to avoid pollution from other fungi. The third group composed of *Cinnamomum camphora* was treated under high-moisture conditions to spontaneously inoculate soft rot fungi. All groups were cultured at the appropriate temperature for 12 weeks to achieve advanced stages of decay (see Figures S4A–S4C).

Charcoalification of modern decay woods

After decay, three groups of rotten wood exhibiting major fungal degradation were prepared for conversion to charcoal. The procedure of charcoalification of decay wood is modified after Moskal-del Hoyo et al. (2010).[10] After the removal of fungal mycelia from the surface of the specimens, the rotten wood samples exhibited specific macroscopic appearances (see Figures S4D–S4F). The infected samples were subsequently cleaned, wrapped in aluminum foil, and placed in capped crucibles to reduce the oxygen supply. All samples were burned at 450°C for 3 h using a muffle furnace. After natural cooling, the laboratory-charcoalified samples were examined under a reflected light microscope

and manually broken. Three sections (transverse, longitudinal-tangential, and longitudinal-radial) were selected and mounted on standard stubs using adhesive tabs. Subsequently, the samples were coated with gold/palladium and later observed under an SU3500 SEM at the Nanjing Institute of Geology and Palaeontology, Chinese Academy of Sciences.

QUANTIFICATION AND STATISTICAL ANALYSIS

The statistical treatment of fossil charcoals from three Permian–Triassic sections were manually performed. From the Lengqinggou Section, a total of 92 rock samples (9 from the coal beds and 83 from the clasolite) were collected to conduct the acid maceration and charcoal fragments were too many to count. In the Dalongkou Section, 89 rock samples were collected mainly from the Guodikeng Formation. As a result, more than 584 pieces of mesoscopic to macroscopic charcoal were obtained. In the Tsaagan Tolgoy Section, totally 86 rock samples were sampled for charcoal extraction and 940 scattered charcoal particles were acquired. The stratigraphical distribution of these charcoal occurrences and the locations of charcoals with wood-decay structures or fungal remains are shown in Figure S2.